Title:

Microbial catabolic and anabolic utilization of hydrocarbons in deep subseafloor sediments of Guaymas Basin

Authors:
Toshiki Nagakura[1] (nagakura@gfz-potsdam.de)
Yuki Morono[2] (morono@jamstec.go.jp)
Motoo Ito[2] (motoo@jamstec.go.jp)
Jens Kallmeyer[1]* (kallm@gfz-potsdam.de)

[1] GFZ German Research Centre for Geosciences, Section 3.7 Geomicrobiology, Telegrafenberg, 14473 Potsdam, Germany
[2] JAMSTEC Japan Agency for Marine-Earth Science and Technology, Kochi Institute for Core Sample Research, 200 Monobe Otsu, 783-8502, Nankoku, Kochi, Japan

*Corresponding author (kallm@gfz-potsdam.de)

This manuscript is a non-peer reviewed preprint submitted to EarthArxiv. This manuscript has not been submitted for publication. Subsequent versions of this manuscript may be slightly different. If accepted, the final-version paper will be available via a “Peer-reviewed publication DOI” link. Please feel free to contact the authors; we welcome feedback.

Microbial catabolic and anabolic utilization of hydrocarbons in deep subseafloor sediments of Guaymas Basin

Toshiki Nagakura[1], Yuki Morono[2], Motoo Ito[2], Jens Kallmeyer[1]*

[1] GFZ German Research Centre for Geosciences, Section 3.7 Geomicrobiology, Telegrafenberg, 14473 Potsdam, Germany

[2] JAMSTEC Japan Agency for Marine-Earth Science and Technology, Kochi Institute for Core Sample Research, 200 Monobe Otsu, 783-8502, Nankoku, Kochi, Japan

*Corresponding author (kallm@gfz-potsdam.de)

Abstract

Guaymas Basin, located off the Gulf of California, is a hydrothermally active marginal basin. Due to steep geothermal gradients and localized heating by sill intrusions, microbial substrates like short-chain fatty acids and hydrocarbons are abiotically produced from sedimentary organic matter at comparatively shallow depths. However, the potential of hydrocarbons as microbial substrates for both catabolic and anabolic metabolism remains elusive. We thus analyzed the effect of hydrocarbons on microbial sulfate reduction rates (SRR) and uptake of hydrocarbons by microorganisms using NanoSIMS. Sediment samples were recovered during IODP Exp. 385. Two sites, U1545C and U1546D, have a distance of roughly 1 km, and their sedimentary sequence and current geothermal gradients are almost identical, but Site U1546D experienced the intrusion of a sill. Since emplacement, the sill has thermally equilibrated with the surrounding sediment. For SRR measurements, sediment samples were amended with four aliphatic and four aromatic hydrocarbons or methane. Incubations were carried out at in-situ temperature and pressure for 10 days. For NanoSIMS analysis, sediment samples were incubated with stable-isotope labeled hydrocarbons (hexadecane-d_{34} + benzene-$^{13}C_6$ or ^{13}C-methane) and $^{15}NH_4Cl$ at in-situ temperature and pressure for 42 days. Our results show that SRR increases upon the addition of either methane and hydrocarbons in samples from near the seafloor at Site U1545C. Methane addition also stimulated SRR around the sulfate-methane transition zone (SMTZ) at Site U1545C. In contrast, SRR did only increase at Site U1546D below the SMTZ, when the sample was incubated with methane, but did not show any reaction on hydrocarbon addition. Despite the relatively short incubation time of only 42 days we succeeded in detecting hydrocarbon and nitrogen uptake in some samples from both sites. Assimilation also mostly occurred in samples near the seafloor. Consequently, these data indicate the potential of microorganisms in Guaymas Basin to metabolize hydrocarbons.

Introduction

The deep subseafloor biosphere harbors vast amounts of prokaryotes, their number is thought to be approximately the same as in soil and seawater (Kallmeyer et al., 2012). In

addition, microorganisms in deep subsurface sediments are metabolically active (D'Hondt et al., 2004; Schippers et al., 2005) or at least revivable (Morono et al., 2011; Trembath-Reichert et al., 2017; Morono et al., 2020). Because of its great amounts of biomass, the deep biosphere is thought to play a vital role in the global cycling of elements (Parkes et al., 2014).

Guaymas Basin, located in the Gulf of California off Mexico, is characterized by strong hydrothermal activity due to seafloor spreading (Kawka and Simoneit 1987). Due to high productivity in its surface waters and in parts high terrigenous sediment input, organic-rich sediment accumulates at rates exceeding 1 mm/year (Calvert 1966; Curray et al., 1979; Teske et al., 2021a). In areas with steep geothermal gradients like Guaymas Basin or Nankai Trough off Japan, bioavailable organic substrates like volatile fatty acids are produced by pyrolysis of macromolecular sedimentary organic matter (kerogen) already at shallow depths (Kawka and Simoneit, 1994; Horsfield et al., 2006; Teske et al., 2014). In addition, laboratory experiments showed that acetate is produced by heating sediment to temperatures in the mesophilic to thermophilic range (Wellsbury et al., 1997). These findings support the notion that in-situ production of organic substrates can support life in the deep subsurface biosphere. The supply of carbon sources in Guaymas Basin is therefore expected to be relatively high and diverse (review in Edgcomb et al., 2022).

Recent technological developments, e.g., deep drilling with contamination control for recovery of samples suitable for microbiological and molecular biological analyses, as well as sensitive techniques e.g. for detections of ultra-low abundances of microbial cells, made it possible to study microbial communities and metabolic activities in the deep biosphere (Colwell and D'Hondt, 2013; Morono and Inagaki, 2016; Kallmeyer, 2017; Morono, 2023). Additionally, to elucidate the metabolic activity of microorganisms in various environments, many molecular biological or chemical analytical techniques are used. Nanoscale secondary ion mass spectrometry (NanoSIMS) is a powerful tool to determine solid surface compositions (e.g., minerals and cells) on the single-cell level because it is capable of nm-scale resolution (e.g., Ito and Messenger, 2008; Kubota et al., 2014; Morono et al., 2020). This technique, therefore, allows analysis of uptake of stable-isotope labeled substrates at the single-cell level (Lechene et al., 2006; Wagner, 2009). NanoSIMS can be combined with fluorescence in-situ hybridization (FISH) for assessment of cellular metabolic activity of specific groups of organisms. Using FISH, Boetius et al., (2000) observed microbial consortia composed of archaea and sulfate-reducing microorganisms that were apparently capable of anaerobic oxidation of methane using sulfate as an electron acceptor. Based on these findings, Orphan et al. (2001) used FISH-NanoSIMS to prove that the archaea actually assimilate methane. However, since marine deep subsurface sediments have very low cell abundances (Parkes et al., 1994; Kallmeyer et al., 2012) and the cells might have low metabolic activity (Schippers et al., 2005), there may only be very few FISH-stained cells and those cells may show only a low signal intensity. Therefore, total cell staining methods like SYBR Green or DAPI staining can be a better or the sole option. Recent studies used NanoSIMS to detect viable cells in coal bed sediment at depths of over 2,000 mbsf (meters below seafloor) (20 million year old) off the Simokita Peninsula, Japan, and in 100 million-year-old sediment of the oligotrophic South Pacific Gyre (Trembath-Reichert et al., 2017;

Morono et al., 2020). Both environments are characterized by extremely low cell abundances and used only SYBR Green staining (10^4 to 10^0 cells cm^{-3} below 1,500 mbsf and 10^6 to 10^2 cells cm^{-3} down to 100 mbsf, respectively) (Inagaki et al., 2015; Trembath-Reichert et al., 2017; Morono et al., 2020).

In anoxic subsurface sediment, after other thermodynamically more efficient electron acceptors (O_2, NO_3^-, Mn(IV), and Fe(III)) are depleted, sulfate reduction becomes the quantitatively dominant organic matter mineralization process (Jørgensen, 1982; Jørgensen, 2000; Parkes et al., 2014). The biodegradation of hydrocarbons under anaerobic conditions and the respective metabolic strategies have already been studied extensively (e.g. Meckenstock and Mouttaki (2011) and references therein). Sulfate reducers can also metabolize a wide variety of carbon sources including aliphatic or aromatic hydrocarbons (Reuter et al., 1994; Coates et al., 1996; Shin et al., 2019). Sulfate reduction fueled by organic matter is commonly termed organoclastic sulfate reduction. Below the zone of organoclastic sulfate reduction, sulfate reduction can be coupled with methane oxidation (methanotrophic sulfate reduction, or anaerobic oxidation of methane; AOM) through a consortium of archaeal methanotrophs and sulfate-reducing bacteria (Iversen and Jorgensen, 1985; Hoehler et al., 1994; Boetius et al., 2000). This process is usually restricted to the relatively narrow depth interval where downward diffusing sulfate and upward diffusing methane overlap, the so-called Sulfate-Methane Transition Zone (SMTZ). Sulfate is not fully depleted in the SMTZ and remains at low µM levels below due to the downward diffusion of sulfide and reoxidation via a cryptic iron-driven sulfur cycle (Holmkvist et al., 2011).

Although pyrolysis of sedimentary organic matter leads to the formation of a wide range of hydrocarbons in Guaymas Basin (Teske et al., 2014), the potential of anabolic and catabolic metabolisms by microorganisms living in these sediments is poorly understood. Our study aims to elucidate anaerobic microbial metabolic activities involving hydrocarbons in Guaymas Basin sediment by addressing the following questions: How much do hydrocarbons influence microbial catabolic activity and which hydrocarbons are assimilated by microorganisms? To address the first question, we quantified the effect of hydrocarbon addition on microbial sulfate reduction via incubation experiments using $^{35}SO_4^{2-}$ radiotracer. The second question is addressed through the detection of uptake of stable isotope-labeled hydrocarbons using NanoSIMS. All incubations were performed at in-situ temperature and pressure.

Materials and Methods

Sampling

The samples were recovered in 2019 during IODP Exp. 385; Guaymas Basin Tectonics and Biosphere (Teske et al., 2021a and Nagakura et al., 2022). For our study, we used cores from sites U1545C and U1546D (Table 1). These two sites are only about 1.1 km apart from each other. Stratigraphy and sediment composition are almost identical at both sites, but sediments at Site U1546D were affected by a sill intrusion. However, since the temperature

gradients at sites U1545C and U1546D are almost identical (225°C/km and 221°C/km, respectively), we can assume that all heat from the sill has already dissipated (Teske et al., 2021a; Nagakura et al., 2022). Table 1 shows the depth and temperature data of the core samples used for this study. The samples were selected from a wide range of temperatures (4°C – 63°C) at similar depths of these two sites. Additionally, we chose one sample from each site that is located near the SMTZ. Samples were stored in nitrogen-filled gas-tight bags at 4°C.

Table 1. Depth and temperature data of the samples from sites U1545C and U1546D. SMTZ at Site U1545C and U1546D are around 40 mbsf and 110 mbsf, respectively. The incubation temperatures were within ±2°C of their in-situ temperatures.

Site U1545C 27°38.2420'N 111°53.3290'W					Site U1546D 27°37.8943'N 111°52.7812'W				
Core number	Depth (mbsf)	In-situ temperature (°C)	Incubation temperature for radioisotope experiment (°C)	Incubation temperature for stable isotope experiment (°C)	Core number	Depth (mbsf)	In-situ temperature (°C)	Incubation temperature for radioisotope experiment (°C)	Incubation temperature for stable isotope experiment (°C)
1	2.0	4.2	4	4	1	2.1	4.3	4	4
6	44.4	13.8	14	15	6	43.8	13.5	14	13
7	54.6	16.1	17	-	14	104.1	26.8	28	-
12	103.9	27.2	28	-	15	114.4	29.1	31	-
14	123.0	31.5	31	32	16	123.8	31.2	31	31
27	185.3	45.5	45	-	23	190.7	46.0	45	-
43	260.7	62.5	63	62	37	261.5	61.7	62	62

Sample preparation

All sample handling was carried out inside a nitrogen-filled anaerobic glovebox. In the anaerobic glovebox, 10 g of sediment was placed into the pre-combusted glass crimp vial at ca. 6°C and mixed with the medium to form a slurry. These procedures were applied to both the radioisotope and stable-isotope experiments described in the following sections. All incubations were carried out at approximate in-situ temperature and pressure (Table 1). During preliminary tests, we realized that particularly at low temperatures the rubber stoppers that close the incubation vials are not flexible enough to transfer the pressure, leading to breaking of incubation vials. Therefore, we cut off the bottom 5 mm of the stoppers to make them thinner and hence more flexible. All materials in contact with the sample were either autoclaved or combusted (400°C for 4 hours).

Radioisotope experiment for the measurements of SRR

In order to quantify the effect of hydrocarbon addition on SRR, we incubated the samples with $^{35}SO_4^{2-}$ radiotracer and a mixture of various hydrocarbons or methane.

Medium preparation

Medium composition and preparation for SRR measurements are the same as in Nagakura et al. (2022): 0.2 g KH_2PO_4, 0.25 g NH_4Cl, 25 g NaCl, 0.5 g $MgCl_2 \times 6H_2O$, 0.5 g KCl, 0.15 g $CaCl_2 \times 2H_2O$, and 0.71 g Na_2SO_4 were mixed with 1 L of MilliQ water. 3 mL of 0.1% resazurin was added to the medium and autoclaved. After autoclaving, 5 mL of Na_2S solution (0.12 g Na_2S in 10 mL MilliQ water) and 5 mL of $NaHCO_3$ solution (0.84 g $NaHCO_3$ in 10 mL MilliQ) were added to the medium after autoclaving and flushed with N_2/CO_2 gas for ca. 2 hrs. The medium was then stored in pre-combusted crimp bottles flushed with N_2/CO_2 gas until use.

Sample preparation and incubation with ^{35}S sulfate and hydrocarbon substrates

We quantified SRR with two different hydrocarbon additions, (a) a mixture of eight hydrocarbons and (b) methane. (a) We prepared eight stock solutions, each containing one hydrocarbon in a concentration of 10% (w/v in acetone) (Widdel and Bak, 1992). The eight stock solutions contained decane, hexadecane, icosane, squalene, benzene, naphthalene, anthracene, and phenanthrene. In the anaerobic glovebox, the medium and 100 µL of each hydrocarbon stock solution were added to the sample vial containing the sediment. The hydrocarbon addition into the sample vial was performed at room temperature to keep hydrocarbons dissolved in acetone. The sample vial was then closed with a black butyl rubber stopper and crimped. Since icosane, anthracene, and phenanthrene did not dissolve completely in acetone, they were added as suspensions. The samples were kept in the anaerobic glovebox overnight at ca. 6°C. (b) For the incubation with methane, the medium was added to the glass vial containing the sample. The sample vial was closed with a black butyl rubber stopper, crimped, and kept in the anaerobic glovebox overnight at ca. 6°C. The next day, a syringe containing 10 mL of methane was stuck into the sample vial. All samples were prepared in duplicates, as triplicates were not possible due to limited amouts of sample material. Table 1 shows the incubation temperature of each sample. Additionally, each run of incubations included killed controls (KCs) and media controls (MCs). KCs were mixed with 20% ZnAc instead of media and either 100 µL of each hydrocarbon stock solution or 10 mL of methane. MCs contained only media. After the pre-incubation, the samples, as well as the KCs and MCs, were injected with 5 MBq $^{35}SO_4^{2-}$ radiotracer and incubated in our high-pressure thermal gradient block (HPTGB) (Kallmeyer et al., 2003; Nagakura et al., 2022) at in-situ temperatures and pressure (ca. 25 MPa) for 10 days. After incubation, the cylinders were depressurized and the sample vials were removed from the cylinders. When the glass vials were opened, the samples were immediately transferred into 50 mL centrifuge tubes containing 5 mL of 20% ZnAc. To transfer the sample and the medium in the vials, the glass vials were rinsed with 10 mL of 20% ZcAc and transferred to the same centrifuge tube to achieve quantitative transfer of the sample. Samples were stored at -20°C until analysis.

Sample distillation and scintillation counting followed by SRR calculation

All inorganic reduced sulfur species (total reduced inorganic sulfur, TRIS), which also contain the microbially produced radiolabeled sulfide, were separated from the sample by cold chromium distillation (Kallmeyer et al., 2004). After thawing the samples, they were centrifuged for 10 min at 2,500 ×g. To quantify the total radioactivity, 50 µL of the

211 supernatant was transferred to a scintillation vial and mixed with 4 mL of scintillation
212 cocktail (Rotiszint® eco plus LSC-Universalcocktail, Carl Roth). The remainder of the
213 supernatant was carefully decanted off and the sediment sample was mixed with 15 mL of
214 *N,N*-Dimethylformamide (DMF) and quantitatively transferred to a glass distillation flask. A
215 magnetic stir bar was put into the flask and set at 400 rpm to ensure complete mixing of the
216 sample and chemicals. The flask was flushed with N_2 to maintain anoxic conditions. After 10
217 min of N_2 flushing, 8 mL of 6N HCl and 15 mL of 1M chromium (II) chloride solution were
218 added through a reaction port to convert all reduced sulfur species in the sediment sample
219 to gaseous H_2S. The H_2S was driven out of the solution by the constant stream of N_2 gas and
220 led through a first trap filled with 7 mL of citric acid solution (19.3 g of citric acid and 4 g of
221 NaOH in 1 L MilliQ water; pH 4) to trap all aerosols potentially containing unreacted ^{35}S-
222 sulfate before reaching a second trap filled with 7 mL of 20% ZnAc solution in which the H_2S
223 is quantitatively converted to solid ZnS. To avoid overflowing of the zinc acetate trap, a few
224 drops of silicon-based antifoam were added. The distillation lasted for 2 hrs. Normally, only
225 5% ZnAc solution is used for the traps, but the amounts of TRIS in the sample requires
226 higher concentrations to ensure the trapping of all sulfide. To avoid the possible
227 interference by high concentrations of acetate with the scintillation cocktail, the 20% ZnAc
228 solution was centrifuged at 2,500 ×g for 10 min and the supernatant was discarded. The ZnS
229 pellet was resuspended with 5% ZnAc and the total volume was adjusted to 7 mL. The ZnS
230 suspension was then quantitatively transferred into a 20 mL plastic scintillation vial and
231 mixed with 8 mL of scintillation cocktail. Distillations were carried out in batches of 10
232 samples plus one distillation blank (DB), containing only a few drops of non-radioactive ZnS
233 carrier. Counter blanks (CBs) contained only 7 mL of 5% ZnAc solution and 8 mL of the
234 scintillation cocktail. MCs and DBs were then directly transferred into plastic scintillation
235 vials and mixed with 8 mL of scintillation cocktail.

236 Radioactivity was quantified using a HIDEX 600 SL Liquid Scintillation Counter (HIDEX Oy)
237 with Guard Scintillator. Before the vials were placed into the counter, they were vortexed to
238 ensure complete mixing of the sample and scintillation cocktail, and the surface of the vial
239 was wiped with a cleaning wipe (Kimtech Science) moistened with 70% ethanol to remove
240 any potential contamination on the surface of the vial.

241 SRR was calculated as follows:

242 $$SRR = (SO_4^{2-})_{TOT} / V_{SED} \times a_{TRIS}/a_{TOT} \times 1/t \times 1.06$$

243 where SRR is calculated in $pmol \cdot cm^{-3} \cdot d^{-1}$, $(SO_4^{2-})_{TOT}$ is the total amount of sulfate in the
244 sample (sulfate in the sediment + sulfate in the medium; pmol), V_{SED} is the volume of the
245 sediment sample (cm^3), a_{TRIS} is the radioactivity of TRIS (Bq), a_{TOT} is the total used
246 radioactivity (Bq), t is the incubation time (d), and the value 1.06 is the correction factor for
247 the isotopic fractionation of sulfur Jørgensen (1978). Since the samples were incubated with
248 media in a slurry, we consider the results as "potential" SRR. The minimum quantification
249 limit (MQL) and minimum detection limit (MDL) were calculated as follows:

250 MDL = Average value of blank a_{TRIS} (KCs, MCs, DBc, and CBs)

MQL = MDL + k × (standard deviation of blank a_{TRIS})

where k is a factor for a confidence level (Kaiser, 1970). k = 3 was applied for the MQL and its confidence level is 95% instead of 99.86% as the blanks are non-normally distributed (Kaiser, 1970). The a_{TRIS} of samples and blanks are compared to determine MDL and MQL.

Stable-isotope experiment for the analysis of hydrocarbon and inorganic nitrogen uptake with NanoSIMS

We aimed to observe hydrocarbon and inorganic nitrogen uptake by incubating sediment samples with stable-isotope-labeled hydrocarbons and ammonium chloride and analyzing them using NanoSIMS.

Medium preparation for stable-isotope analyses

The composition of the medium was the same as in Nagakura et al. (2022), but slightly modified for the stable isotope uptake analysis with NanoSIMS; 0.2 g KH_2PO_4, 0.225 g $^{14}NH_4Cl$, 0.025 g $^{15}NH_4Cl$ (for nitrogen uptake analysis), 25 g NaCl, 0.5 g $MgCl_2 \times 6H_2O$, 0.5 g KCl, 0.15 g $CaCl_2 \times 2H_2O$, and 0.71 g Na_2SO_4 mixed with 1 L of MilliQ water. 3 mL of 0.1% resazurin was added to the medium and autoclaved. 5 mL of Na_2S solution (0.12 g Na_2S in 10 mL MilliQ water) and 5 mL of $NaHCO_3$ solution (0.84 g $NaHCO_3$ in 10 mL MilliQ water) were added to the medium after autoclaving and flushed with N_2/CO_2 gas for ca. 2 hrs. The medium was then stored in autoclaved serum bottles flushed with N_2/CO_2 gas until use.

Sample incubation with stable isotope substrates

Similar to the SRR measurements, we separated the samples for quantification of anabolic activity (i.e., uptake) via NanoSIMS into two groups, (a) uptake of benzene and hexadecane and (b) uptake of methane. Both types of samples were amended with ^{15}N-ammonium chloride to monitor uptake of inorganic nitrogen. (a) Each 10% (w/v of acetone) hydrocarbon stock solution (hexadecane and benzene) was prepared (Widdel and Bak, 1992). The hexadecane stock solution consisted of 90wt% of normal hexadecane and 10wt% of fully deuterated hexadecane-d_{34}. The benzene stock solution consisted of 80wt% of benzene and 20wt% of benzene-$^{13}C_6$. When the medium was added to the glass vial containing the sample, 400 µL of each hydrocarbon stock solution was added as well, and the sample vial was closed with a black butyl rubber stopper and crimped. The stock solutions were added to the sample vials at room temperature to keep the hydrocarbons dissolved in acetone. In addition, a 3 mL syringe including 0.5 mL of the medium was stuck into each vial to avoid breakage of the glass vial upon pressurization. The samples were pre-incubated overnight in the anaerobic glovebox to allow the microorganisms to adjust to the new condition. (b) For the incubation with methane, the sediment samples were mixed with the medium and pre-incubated in the anaerobic glovebox overnight. After pre-incubation, 10 mL of gaseous methane, consisting of 80v% ^{12}C-methane and 20v% of ^{13}C-methane was injected into the sample vial. For both types of incubations we also prepared two killed controls (KCs), which were mixed with 20% ZnAc instead of media. Other conditions were

290 the same as the samples mentioned above; one KC was prepared with hydrocarbons (a),
291 and the other one with methane (b).

292 The samples were put into high-pressure cylinders and they were incubated in a HPTGB
293 system (Kallmeyer et al., 2003; Nagakura et al., 2022) at in-situ temperature (Table 1) and
294 pressure (ca. 25 MPa) for 42 days.

295 *Sample fixation*

296 At the end of the incubation, samples were fixed in Phosphate-Buffered Saline (PBS)
297 solution and paraformaldehyde (PFA) solution. The solutions were prepared as 10X PBS and
298 9.33% PFA. For 10X PBS solution, 79.4 g NaCl, 1,9 g KCl, 11.4 g Na_2HPO_4, and 2.6 g KH_2PO_4
299 were mixed in 1 L MilliQ (pH 7.2). The solution was then autoclaved and stored at room
300 temperature. For 9.33% PFA solution, 28 g of PFA was added to 260 mL MilliQ water and
301 heated at ca. 60°C. As PFA only dissolves in alkaline conditions, 1N NaOH was added until
302 the PFA was dissolved. The solution was then cooled down and 30 mL of 10X PBS was
303 added. HCl was added to adjust the pH to 7.2. To maintain consistent osmotic conditions,
304 we also added 5.1 g NaCl. The solution was brought to its final volume of 300 mL by adding
305 MilliQ water, then the solution was sterile filtered (0.2 µm pore size). When the PFA solution
306 is mixed with the incubation media, it has a final concentration of ca. 4%.

307 Upon removal of the samples from the HPTGB the sample vials were opened and the
308 sediment and medium immediately transferred into 50 mL centrifuge tubes including 15 mL
309 of 9.33% PFA solution and stored for 22 hrs at 4°C. After this fixation step, the samples were
310 centrifuged at 2,500 x g for 15 min and the supernatant was discarded. Afterwards, the
311 samples were washed twice with 1X PBS. Once the samples were fixed, they were preserved
312 in PBS/ethanol (1:1 [v/v]) and kept at -20°C until analysis at JAMSTEC in Kochi, Japan.

313 *Cell detaching and sorting*

314 At JAMSTEC, the following procedures were performed for detaching cells from sediments.

315 1. 0.5 mL of the sample slurries were transferred into new 15 mL centrifuge tubes and
316 mixed with 1 mL of 2.5% NaCl.
317 2. Samples were centrifuged at 5,000 ×g for 10 min and the supernatants were discarded.
318 3. The sediment pellets were mixed with 2.7 mL of pre-filtered 3X PBS, 0.5 mL NaCl, 0.4
319 mL detergent mix (Kallmeyer et al., 2008), and 0.4 mL methanol.
320 4. The suspensions were shaken at 500 rpm for 1 hour with a shaker (ShakeMaster, bms
321 biomedical science), followed by sonication (Bioruptor, Cosmo Bio Co., Ltd.) for 20 min
322 (20 cycles of sonication at 200 W for 30-sec with 30-sec intervals).
323 5. The samples were carefully put onto the top surface of the following density gradient
324 containing the following solutions: from surface to bottom in 15 mL centrifuge tubes; 4
325 mL of 30% [v/v] Nycodenz, 4 mL of 50% [v/v] Nycodenz, 4 mL of 80% [v/v] Nycodenz,
326 and 4 mL of 67% [v/v] sodium polytungstate.
327 6. The tube was centrifuged for 1 hour at 10,000 ×g and 4°C.
328 7. The supernatants were collected and transferred into new 15 mL centrifuge tubes.
329 8. 5 mL of NaCl was added to the sediment and resuspended.

9. The slurry was centrifuged at 6,000 ×g for 15 min and the supernatant was discarded.
10. The rest was mixed with 2.2 mL of NaCl, 0.4 mL of D-mix, and 0.4 mL of methanol.
11. The mixed solution was shaken at 500 rpm for 10 min.
12. The sample was then sonicated for 20 min.
13. The sample was placed gently onto the gradient layer solution in 15 mL centrifuge tubes.
14. The tube was centrifuged at 10,000 ×g for 1 hour.
15. The supernatant was carefully recovered and stored with the supernatant collected before.

The cells in the supernatant were collected by filtration through an Anodisc™ 25 aluminum oxide filter (pore size 0.2 µm). Five hundred microliter of 1X TE buffer was also placed on Anodisc to wash out the density gradient compounds. After removing the solution and stopping the vacuum pump, 110 µL of 40X diluted SYBR Green I (Thermo Fischer Scientific) was immediately put onto the filter and left for 10 min. After 10 min, 500 µL of 1X TE buffer was poured onto the Anodisc membrane while vacuuming to wash the membrane. Right after the final drop of the liquid had passed through the membrane, the membrane was immediately put in a 50 mL centrifuge tube containing 5 mL of 1X TE buffer, placing the side containing the cells facing down. The tube containing the filter was then sonicated twice for 30 sec each at 200W. Then the suspension was stored at 4°C.

The stained cells were sorted by a cell sorter (MoFlo XDP, Beckman Coulter). Cells were directly sorted onto an indium tin oxide (ITO)-coated membrane. Approximately 10,000 cells were sorted on the ITO membrane. For the sample from Site U1545 Core 16 incubated with benzene and hexadecane, 30,000 cells were sorted. The area where the cells were sorted was marked by laser microdissection (LMD6000; Leica Microsystems).

Analysis of hydrocarbon uptake with NanoSIMS

The sorted microbial cells on an ITO-coated membrane were analyzed with the JAMSTEC NanoSIMS 50L ion microprobe (AMETEK Co. Ltd, CAMECA BU). The samples incubated with benzene and hexadecane, $^{1}H^{-}$ and $^{2}H^{-}$ were analyzed as well after the analysis of carbon and nitrogen isotopes. The analytical procedures were described elsewhere (e.g., Morono et al., 2020). In brief, a focused primary positive Cs ion beam of approximately ~1.5 pA was used for carbon and nitrogen isotopic analyses, and approximately ~6 pA was used for hydrogen isotopic analysis, rastered over 24 × 24 µm areas on the samples. Each analysis was initiated after stabilization of the secondary ion beam intensity following several minutes of pre-sputtering with a relatively strong primary ion beam current (~20 pA). For carbon and nitrogen isotopic analysis, images of $^{12}C^{-}$, $^{13}C^{-}$, $^{16}O^{-}$, $^{12}C^{14}N^{-}$, $^{12}C^{15}N^{-}$, and $^{32}S^{-}$ were acquired simultaneously in multidetection with six electron multipliers (EMs) at a mass resolving power of approximately 9000, sufficient to separate all relevant isobaric interferences ($^{12}C^{1}H$ on ^{13}C and $^{13}C^{14}N$ on $^{12}C^{15}N$). For hydrogen isotopic analysis, images of $^{1}H^{-}$, $^{2}H^{-}$, and $^{12}C^{-}$ were acquired using three EMs in multidetection mode at a mass resolving power of approximately 3000. Each analysis consisted of the same area, which individual images consisting of 256 × 256 pixels. The dwell times were 2 ms/pixel (131.072 sec/scan) for the

carbon and nitrogen isotopic analyses and 5 ms/pixel (327.68 sec/scan) for the hydrogen isotopic analysis.

Examination of isotope abundance ratio with OpenMIMS

After the NanoSIMS analysis was performed, the data was saved in IM files. To open and see the NanoSIMS images, the OpenMIMS plugin in the application ImageJ of Fiji software was used. Each of the vertically stacked spattered planes, analyzed with NanoSIMS, was aligned to correct the drift during the acquisition of each plane image and integrated into an image.

To identify the cellular regions analyzed with NanoSIMS, the NanoSIMS images were compared to the fluorescence microscopy images which were taken before (Figure 1). We were able to match the isotope images and the fluorescence microscopy image in about half of the samples.

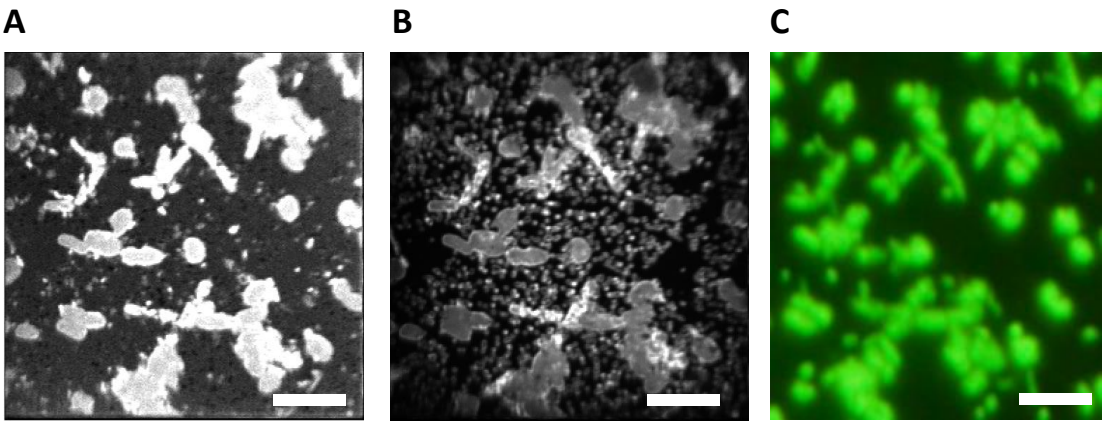

Figure 1: NanoSIMS isotope images and fluorescence microscopy images of the sample Core 6 at Site U1546D, incubated with methane. A: ^{12}C isotope images analyzed with NanoSIMS. B: $^{12}C^{14}N$ isotope images analyzed with NanoSIMS. C: Fluorescence microscopy images. The cells were dyed with SYBR Green I. Scale bars in each panel represent 5 µm.

Cells shown in the isotope images were marked as regions of interest (ROI) and the isotope abundance of each ROI was thereby calculated. $^{13}C/(^{12}C+^{13}C)$, $^{12}C^{15}N/(^{12}C^{14}N+^{12}C^{15}N)$, or $^{2}H/(^{1}H+^{2}H)$ isotope abundance ratios were calculated to examine if the cells assimilated the isotopes. ROI were drawn based on the following criteria: (1) ROI were drawn based on the clear isotope signals in ^{12}C images. When the signals are clearly detected, ROI were drawn also based on the ^{13}C images or $^{12}C/^{15}N$ images (heavy isotope images). (2) If at least one of the isotope abundance ratios was zero, the ROI was excluded. These criteria were also applied to the samples matching the NanoSIMS and the fluorescence microscopy images.

Since the calculated values are not absolute values but relative values, the ROI in each analysis were standardized by the "blank" ROI drawn at a membrane region without any cells. This blank region is regarded as the natural abundance ratio of each isotope ($^{13}C/(^{12}C+^{13}C)$ = 1.06%, $^{15}N/(^{14}N+^{15}N)$ = 0.4%, and $^{2}H/(^{1}H+^{2}H)$ = 0.0115%; Trivedy et al., 2016).

The isotope abundance ratios were calculated as follows (here presented for carbon as an example).

$$\text{Isotope abundance ratio (C, \%)} = {}^{13}C/({}^{12}C+{}^{13}C) \times 100$$

This calculation was also done for the KCs to obtain the average and standard deviation values for the statistical threshold.

Statistical threshold (-) = (Average of the isotope abundance ratio of KC) + 3 × (Standard deviation of the isotope abundance ratio of KC)

This calculation assumes that the ROI values of KCs are normally distributed. The values were then converted to the isotope abundance ratios and described in percentages.

Results

SRR and the addition of hydrocarbons

We measured SRR in samples from both sites, U1545C and U1546D, covering a wide depth and temperature range (from 2 mbsf to 261 mbsf; from 4°C to 63°C) (Figure 2). The study of Nagakura et al. (2022) presented SRR measured on the same samples but without hydrocarbon additions. At Site U1545C, SRR increased upon the addition of methane and the hydrocarbon mixture in the shallowest sample (Core 1, 2 mbsf) (Figure 2A). In Core 6 and 7 from near the SMTZ (44 mbsf and 55 mbsf, respectively), SRR increased upon the addition of methane, representing the increase of methanotrophic sulfate reduction (AOM), but not when adding the hydrocarbon mixture. In samples from below the SMTZ SRR did not increase at Site U1545C. At Site U1546D SRR did not increase at all upon hydrocarbon addition (Figure 4B). However, in Core 23 (191 mbsf) below the SMTZ, SRR were recorded above MQL upon the addition of methane, whereas all SRR fell below MQL in previous incubations without any substrate additions.

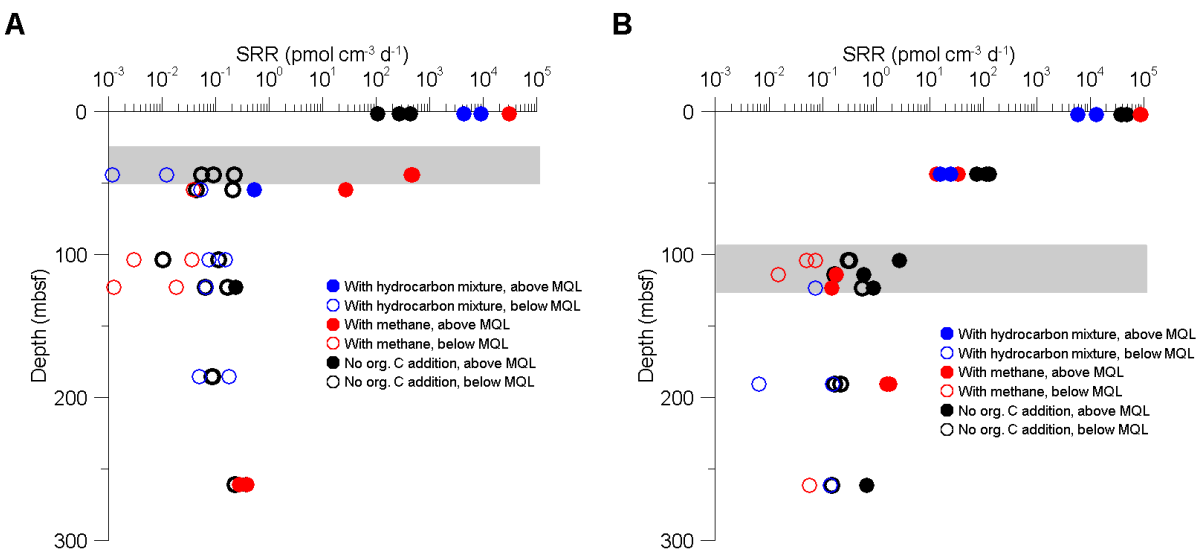

Figure 2: A: SRR at Site U1545C. B: SRR at Site U1546D. Blue circles show SRR measured from the samples incubated with the hydrocarbon mixture, and red circles show SRR measured from the samples incubated with methane. Black circles show SRR measured from the samples incubated without any substrate addition (Nagakura et al., 2022). Solid circles indicate SRR > MQL and open circles indicate SRR < MQL. Gray bars indicate the depth of the respective SMTZ (ca. 40 mbsf and ca. 110 mbsf). A few data points are missing due to the loss of vials during incubation. Due to the lack of sediment, these experiments could not be repeated. All incubations were carried out at in-situ temperature and pressure.

Detection of hydrocarbon and inorganic nitrogen uptake with NanoSIMS

We compared hydrocarbon uptake in the incubated samples with those from the KCs to determine if the uptake is statistically significant (Figure 3). The vast majority of the ROI indicates no uptake of carbon compounds (Figure 3A and B). However, a few ROI indicate low levels of benzene uptake (Figure 3A) and visible uptake of carbon from methane (Figure 3B).

Nitrogen from ammonium chloride was assimilated in almost all samples, especially in Core 1 and Core 6 from Site U1546D in incubations with methane (Figure 3C and D). The highest isotope abundance ratio of Core 1 from Site U1546D incubated with methane reaches more than 8%. The median isotope abundance ratio of ROI of Core 6 from Site U1546D incubated with methane shows about 4%.

The uptake of hexadecane was observed by deuterium incorporation (Figure 3E). The isotope abundance ratio of Site U1545C apparently decreases with depth and hence temperature, though only comparatively few ROI are above the statistically significant value.

Overall, the results show the uptake of hydrocarbons (benzene, hexadecane, and methane) and inorganic nitrogen (ammonium chloride).

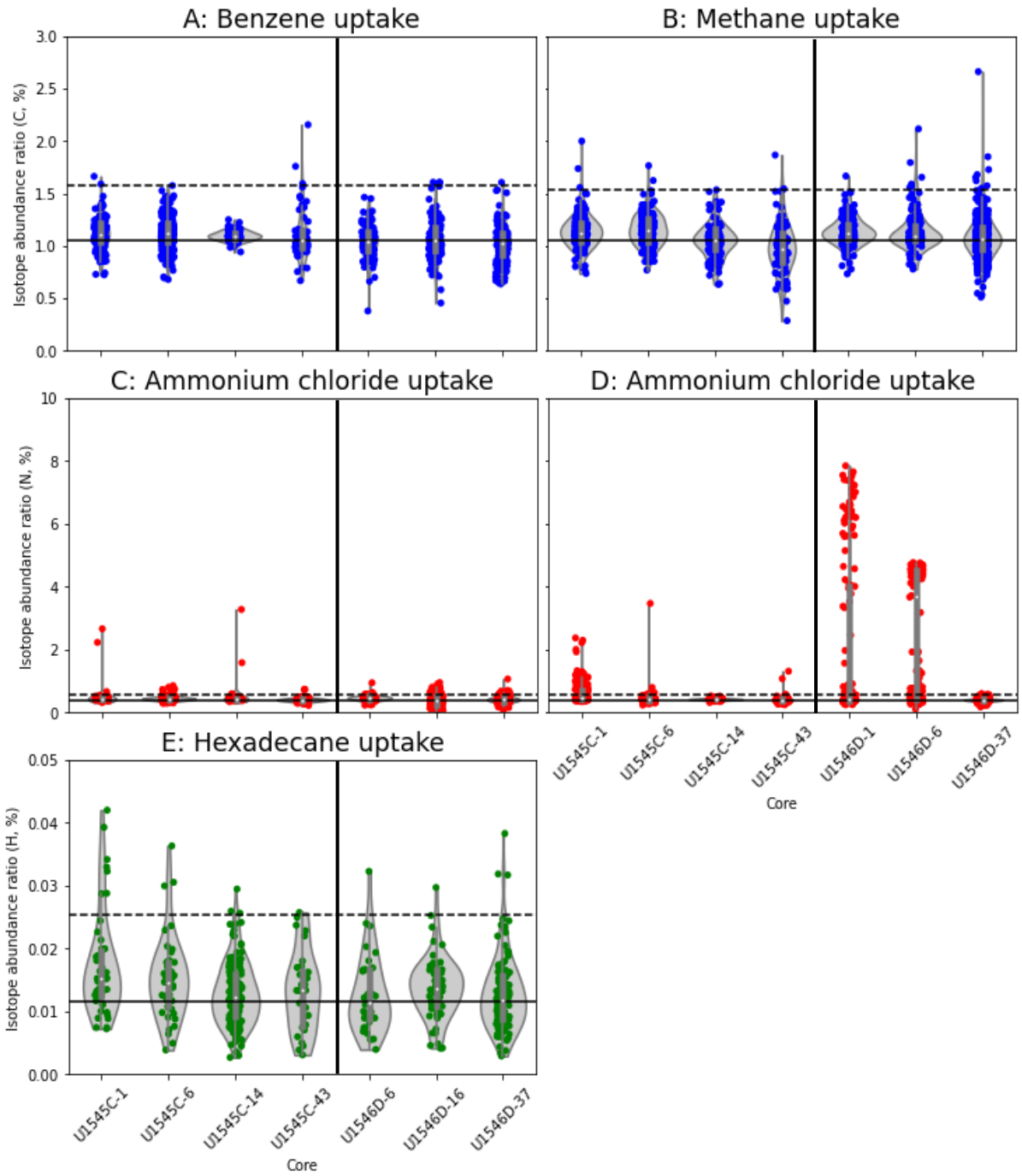

Figure 3: Isotope abundance ratios of each sample. A and B: Carbon uptake from benzene (A) and methane (B). C and D: Nitrogen uptake from ammonium chloride. E: Deuterium uptake from hexadecane. A, C, and E: Samples incubated with benzene and hexadecane. B and D: Samples incubated with methane. KCs were incubated with ^{15}N-ammonium chloride plus either with benzene and hexadecane (A, C, E) or with methane (B, D). Black solid lines represent the natural incorporation ratios of each isotope (Carbon = 1.06%, Nitrogen = 0.4%, and Hydrogen = 0.0115%, respectively). Black dashed lines represent the statistical threshold values of the uptake of respective isotopes (A, C, E: Carbon = 1.58%, Nitrogen = 0.58%, and Hydrogen = 0.0255%, respectively; B, D: Carbon = 1.54%, and Nitrogen = 0.57%, respectively). See the method section for more details. A few data are missing due to the

breaking of vials during incubation and the lack of additional sediment to repeat the experiments. Note the different ranges of isotope abundance ratios of each element on the y-axes.

Since $^{13}C/(^{12}C+^{13}C)$ and $^{12}C^{15}N/(^{12}C^{14}N+^{12}C^{15}N)$ were measured separately from $^{2}H/(^{1}H+^{2}H)$, we tried to match the ROI to those based on the carbon, nitrogen, and hydrogen isotope images as much as possible. Based on the position of cells in each isotope image, the cells were manually matched to each other and summarized in the 3D plot (Figure 4). The figure summarizes only the results from the samples incubated with benzene and hexadecane as the samples incubated with methane were not incubated with a ^{2}H-labeled substance.

Our results indicate that there is no simultaneous uptake of different isotope-labeled compounds. Benzene uptake is less than hexadecane and ammonium chloride uptake, and the samples from near the seafloor tend to have higher incorporation ratios than those from deeper cores (Figure 3 and 4). There are two remarkable signals from Site U1545C Core 1 (Figure 4A). One shows a high nitrogen isotope abundance ratio (≈ 2.67%) and another shows a high hydrogen isotope abundance ratio (≈ 0.0420%).

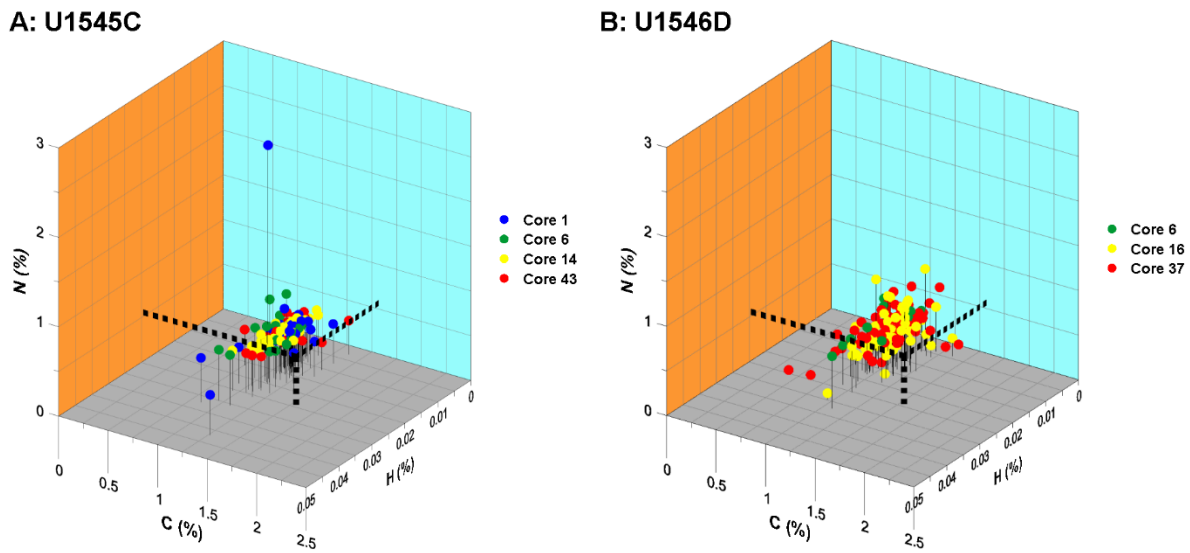

Figure 4: 3D plots of isotope abundance ratios for carbon (benzene), nitrogen (ammonium chloride), and hydrogen (hexadecane) uptake. A: Site U1545C and B: Site U1546D. Red dashed lines represent the thresholds for each element (C = 1.58%, N = 0.584%, and H = 0.0255%), above which incorporation becomes statistically significant corresponding to Figure 3.

Discussion

Relation between the assimilation of organic/inorganic matter and dissimilatory sulfate reduction

Hexadecane was taken up more than benzene and the uptake tends to decrease with depth (Figure 3A and E). This may be because of the different biodegradability between these two compounds. Hexadecane is a linear and non-branched aliphatic hydrocarbon and can be degraded more easily by microorganisms than benzene (Edgcomb et al., 2022), which is a more stable and recalcitrant aromatic hydrocarbon.

In samples from Site U1546D Core 1 and 6, nitrogen (from ammonium chloride) and methane were assimilated (Figure 3D), but SRR did not increase with the addition of methane (Figure 2B). We interpret this observation as sulfate-reducing microorganisms being active but they did not use methane because of the abundance of more favorable organic compounds produced by pyrolysis, which was triggered by the sill (Teske et al., 2014), even though the heating from the sill at Site U1546D has already ceased (Teske et al., 2021a; Nagakura et al., 2022). Other electron acceptors such as NO_3^-, Mn(IV), or Fe(III) can contribute to the assimilation, but these electron acceptors are depleted and hence not available (LIMS Reports: https://web.iodp.tamu.edu/LORE/). Compared to hydrocarbons (benzene and hexadecane), ammonium chloride uptake was higher in these cores, suggesting nitrogen is limited in these deep subsurface sediments or inorganic nitrogen is taken up faster than hydrocarbons. This result concurs with Trembath-Reichart et al. (2017) in which ^{15}N-ammonium and ^{15}N-methylamine were incorporated although ^{13}C-methanol and ^{13}C-methylamine uptake was not observed, and Morono et al. (2020) in which nitrogen incorporation was much more observed in first 21 days and thereafter (day 68 and 557).

However, the nitrogen uptake was less in the sample Core 6 at Site U1546D when the sediment was incubated with a mixture of hydrocarbons (benzene and hexadecane) (Figure 3C), as compared to the same sample incubated with methane (Figure 3D). This might be either methane stimulated nitrogen uptakers or benzene/hexadecane suppressed nitrogen uptakers. Although this is still elusive, nitrogen uptake by microorganisms in deep subsurface sediments is well-documented (Morono et al., 2011; Trembath-Reichart et al., 2017; Morono et al., 2020). According to the works by Kellermann et al. (2012), inorganic carbon (bicarbonate) is taken up preferentially over methane, but methane is used as an energy source.

The studies of Trembath-Reichart et al. (2017) and Morono et al. (2020), in which microorganisms recovered from deep subsurface sediments were incubated for much longer, i.e., months to several years, showed significant microbial uptake of ^{2}H-, ^{13}C-, ^{15}N-labeled substrates. Morono et al., (2020) demonstrated also uptake of carbon in 21 days but the substrates were more favorable (e.g., acetate and pyruvate; volatile fatty acids) and incubations were carried out with aerobic organisms, having thermodynamically more efficient metabolisms. Although our samples were incubated for only 42 days, which was relatively short, and the added carbon sources were hydrocarbons, uptake of hydrocarbons was successfully observed. To observe a higher degree of assimilation, a longer incubation time would be needed.

Anaerobic degradation of hydrocarbons and sulfate-reducing microorganisms

It has been already known for decades that sulfate-reducing microorganisms can degrade both aliphatic and aromatic hydrocarbons under anaerobic conditions (e.g. Rueter et al., 1994, Meckenstock and Mouttaki (2011) and references therein). Despite their stability, sulfate-reducing microorganisms can degrade the aromatic hydrocarbons used in this study: benzene (Edwards and Grbić-Galić, 1992; Lovley et al., 1995; Anderson and Lovley, 2000), naphthalene (Zhang and Young, 1999; Meckenstock et al., 2000; Musat et al., 2009), phenanthrene (Zhang and Young, 1999; Ramsay et al., 2003; Davidova et al., 2007; Tsai et al., 2009), and anthracene (Ramsay et al., 2003). Therefore, we assume that the increase in SRR was induced by one or several of the added aliphatic/aromatic hydrocarbons. With the exception of methane, all hydrocarbons were added simultaneously, so it is not possible to identify which one was used for dissimilatory sulfate reduction.

Because microbial sulfate reduction is a catabolic process and more exergonic than hydrocarbon uptake, which is an anabolic process, it can be measured in a shorter time. Some anabolic processes of microorganisms including ammonia oxidizers, methanotrophs, sulfate oxidizers, and sulfate reducers are assumed even endergonic, although it depends on the conditions (Allen et al., 2023). Trembath-Reichart et al. (2017), for example, carried out anabolic process experiments using anoxic sediments from off Shimokita peninsula, Japan and incubated those samples for 2.5 years to reach a detectable signal of incorporation, while our SRR data was measurable after incubation for 10 days. The samples from Site U1546D showed a less positive response to the hydrocarbon addition in terms of SRR, as compared to the samples from Site U1545C (Figure 2). This may be because the sulfate-reducing microorganisms at Site U1546D did not metabolize as much added hydrocarbons as the sulfate-reducing microorganisms at Site U1545C, although cell abundances between these two sites are similar (~10^9 cells cm^{-3} near the seafloor to ca. 10^6 cells cm^{-3} around 175 mbsf) (Teske et al., 2021b; Teske et al., 2021c). One possible explanation for these findings might be related to the sill emplaced at Site U1546D. Upon heating, macromolecular sedimentary organic carbon will be pyrolyzed and converted into bioavailable organic substrates (Horsfield et al., 2006), so the input of heat into the sediment by the emplacement of the sills (Teske et al., 2014), might have increased the availability of the microbial substrates. Given the overall low microbial activity in these sediments, especially at greater depths, and the heat sterilization of the sediment around the intruded sill as well as the subsequent recolonization of the sediment, the microbial substrates that were produced by thermal cracking might be still available in the sediment, even though the heat effect of the sill at Site U1546D has already ceased. The extent of the thermal aureole and hence the sterilized zone is still unknown. However, it is estimated that 3.3 Mt of carbon were released by this sill intrusion (Lizarralde et al., 2023). If those thermogenically produced bioavailable carbon sources still existed in the sediment, providing a reservoir of readily bioavailable substrates and thus the hydrocarbons added in this experiment were not utilized and did not increase SRR. Given the lack of thermogenically produced substrates at Site U1545C, the microorganisms metabolized the added hydrocarbons instead. Edgcomb et al. (2022) argue that linear aliphatic hydrocarbons, such as decane and hexadecane are easier to degrade than recalcitrant polycyclic ones (naphthalene, anthracene, and phenanthrene). Combining this argument with our SRR data (Figure 2A) and with the

anabolic data (Figure 3A and E) from our NanoSIMS analyses, we argue that microorganisms can utilize hydrocarbons catabolically and anabolically but use them preferentially for catabolism.

Summary

Microbial catabolic and anabolic utilization of various hydrocarbons in hydrothermally influenced subsurface sediments of Guaymas Basin were analyzed using radioisotope- and stable-isotope-labeled compounds. Radioisotope experiments showed an increase in SRR in samples from near the seafloor at Site U1545C upon the addition of hydrocarbons, whereas SRR did not increase in most samples from Site U1546D. This may infer that at Site U1546D more favorable carbon compounds that were produced when the sill had been active, are still available. NanoSIMS analysis revealed the uptake of carbon from benzene and methane and hydrogen from hexadecane by microorganisms in a relatively short incubation time of 42 days. Nitrogen uptake from ammonium chloride was recorded especially from Core 1 and 6 at Site U1546D, incubated together with methane, indicating the presence of active hydrocarbon-metabolizing processes. To sum up, microorganisms in Guaymas Basin have the potential to utilize hydrocarbons buried in Guaymas Basin for both anabolism and catabolism.

Funding

TN is funded through a DFG grant to JK (grant #670521). TN's research travel to JAMSTEC was funded by an ECORD Research Grants 2021 for Early Career Scientists awarded to TN.

Acknowledgments

We thank Andreas Teske and Kai Mangelsdorf who advised us on the usage of hydrocarbons for the experiment of SRR measurements, Virginia Edgcomb and Paraskevi Mara who provided us the hydrocarbon data of Guaymas Basin. Jan Axel Kitte and Simone Bernsee helped with the radioisotope experiments. Zeyu Jia and Seyma Özcirak Ergün advised TN on the protocol of the cell fixation. Takeshi Terada helped with the flow cytometry. The members of the Geomicrobiology group at JAMSTEC; Harumi Isshiki, Fumiaki Mori, and Tomoyasu Nishimura advised and helped during TN's stay in Kochi, Japan.

Reference

Alkorta, I. and J. Elguero (2006). "The carbon–carbon bond dissociation energy as a function of the chain length." Chemical Physics Letters **425**(4): 221-224.

Allen, B., R. Gonzalez-Cabaleiro, I. D. Ofiteru, L. Øvreås, W. T. Sloan, D. Swan and T. Curtis (2023). "Diversity and metabolic energy in bacteria." FEMS Microbiology Letters **370**.

Anderson, R. T. and D. R. Lovley (2000). "Anaerobic Bioremediation of Benzene under Sulfate-Reducing Conditions in a Petroleum-Contaminated Aquifer." Environmental Science & Technology **34**(11): 2261-2266.

Boetius, A., K. Ravenschlag, C. J. Schubert, D. Rickert, F. Widdel, A. Gieseke, R. Amann, B. B. Jørgensen, U. Witte and O. Pfannkuche (2000). "A marine microbial consortium apparently mediating anaerobic oxidation of methane." Nature **407**(6804): 623-626.

Calvert, S. (1966). "Accumulation of diatomaceous silica in the sediments of the Gulf of California." Geological Society of America Bulletin **77**(6): 569-596.

Coates, J. D., R. T. Anderson and D. R. Lovley (1996). "Oxidation of Polycyclic Aromatic Hydrocarbons under Sulfate-Reducing Conditions." Applied and Environmental Microbiology **62**(3): 1099-1101.

Colwell, F. S. and S. D'Hondt (2013). "Nature and Extent of the Deep Biosphere." Reviews in Mineralogy and Geochemistry **75**(1): 547-574.

Curray, J., D. Moore, E. Aguayo, M. Aubry, G. Einsele, D. Fornari, J. Gieskes, J. Guerrero, M. Kastner and K. Kelts (1979). "Leg 64 seeks evidence on development of basins." Geotimes **24**(7): 18-20.

Davidova, I. A., L. M. Gieg, K. E. Duncan and J. M. Suflita (2007). "Anaerobic phenanthrene mineralization by a carboxylating sulfate-reducing bacterial enrichment." The ISME Journal **1**(5): 436-442.

D'Hondt, S., B. B. Jørgensen, D. J. Miller, A. Batzke, R. Blake, B. A. Cragg, H. Cypionka, G. R. Dickens, T. Ferdelman and K.-U. Hinrichs (2004). "Distributions of microbial activities in deep subseafloor sediments." Science **306**(5705): 2216-2221.

Edgcomb, V. P., A. P. Teske and P. Mara (2022). "Microbial Hydrocarbon Degradation in Guaymas Basin-Exploring the Roles and Potential Interactions of Fungi and Sulfate-Reducing Bacteria." Frontiers in microbiology **13**: 831828-831828.

Edwards, E. A. and D. Grbić-Galić (1992). "Complete mineralization of benzene by aquifer microorganisms under strictly anaerobic conditions." Applied and Environmental Microbiology **58**(8): 2663-2666.

Hoehler, T. M., M. J. Alperin, D. B. Albert and C. S. Martens (1994). "Field and laboratory studies of methane oxidation in an anoxic marine sediment: Evidence for a methanogen-sulfate reducer consortium." Global Biogeochemical Cycles **8**(4): 451-463.

Holmkvist, L., T. G. Ferdelman and B. B. Jørgensen (2011). "A cryptic sulfur cycle driven by iron in the methane zone of marine sediment (Aarhus Bay, Denmark)." Geochimica et Cosmochimica Acta **75**(12): 3581-3599.

Horsfield, B., H. J. Schenk, K. Zink, R. Ondrak, V. Dieckmann, J. Kallmeyer, K. Mangelsdorf, R. di Primio, H. Wilkes, R. J. Parkes, J. Fry and B. Cragg (2006). "Living microbial ecosystems within the active zone of catagenesis: Implications for feeding the deep biosphere." Earth and Planetary Science Letters **246**(1): 55-69.

Inagaki, F., K.-U. Hinrichs, Y. Kubo, M. W. Bowles, V. B. Heuer, W.-L. Hong, T. Hoshino, A. Ijiri, H. Imachi, M. Ito, M. Kaneko, M. A. Lever, Y.-S. Lin, B. A. Methé, S. Morita, Y. Morono, W. Tanikawa, M. Bihan, S. A. Bowden, M. Elvert, C. Glombitza, D. Gross, G. J. Harrington, T. Hori, K. Li, D. Limmer, C.-H. Liu, M. Murayama, N. Ohkouchi, S. Ono, Y.-S. Park, S. C. Phillips, X. Prieto-Mollar, M. Purkey, N. Riedinger, Y. Sanada, J. Sauvage, G. Snyder, R. Susilawati, Y. Takano, E. Tasumi, T. Terada, H. Tomaru, E. Trembath-Reichert, D. T. Wang and Y. Yamada (2015). "Exploring deep microbial life in coal-bearing sediment down to ~2.5 km below the ocean floor." Science **349**(6246): 420-424.

Ito, M. and S. Messenger (2008). "Isotopic imaging of refractory inclusions in meteorites with the NanoSIMS 50L." Applied Surface Science **255**(4): 1446-1450.

Iversen, N. and B. B. Jorgensen (1985). "Anaerobic methane oxidation rates at the sulfate-methane transition in marine sediments from Kattegat and Skagerrak (Denmark) 1." Limnology and Oceanography **30**(5): 944-955.

Jørgensen, B. B. (1978). "A comparison of methods for the quantification of bacterial sulfate reduction in coastal marine sediments." Geomicrobiology Journal **1**(1): 11-27.

Jørgensen, B. B. (1982). "Mineralization of organic matter in the sea bed—the role of sulphate reduction." Nature **296**(5858): 643-645.

Jørgensen, B. B. (2000). Bacteria and marine biogeochemistry. Marine geochemistry, Springer**:** 173-207.

Kaiser, H. (1970). "Report for analytical chemists. II. Quantitation in elemental analysis." Analytical Chemistry **42**(4): 26A-59a.

Kallmeyer, J., T. G. Ferdelman, K.-H. Jansen and B. B. Jørgensen (2003). "A high-pressure thermal gradient block for investigating microbial activity in multiple deep-sea samples." Journal of Microbiological Methods **55**(1): 165-172.

Kallmeyer, J., T. G. Ferdelman, A. Weber, H. Fossing and B. B. Jørgensen (2004). "A cold chromium distillation procedure for radiolabeled sulfide applied to sulfate reduction measurements." Limnology and Oceanography: Methods **2**(6): 171-180.

Kallmeyer, J., D. C. Smith, A. J. Spivack and S. D'Hondt (2008). "New cell extraction procedure applied to deep subsurface sediments." Limnology and Oceanography: Methods **6**(6): 236-245.

Kallmeyer, J., R. Pockalny, R. R. Adhikari, D. C. Smith and S. D'Hondt (2012). "Global distribution of microbial abundance and biomass in subseafloor sediment." Proceedings of the National Academy of Sciences **109**(40): 16213-16216.

Kallmeyer, J. (2017). "Contamination control for scientific drilling operations." Advances in applied microbiology **98**: 61-91.

Kawka, O. E. and B. R. T. Simoneit (1987). "Survey of hydrothermally-generated petroleums from the Guaymas Basin spreading center." Organic Geochemistry **11**(4): 311-328.

Kawka, O. E. and B. R. T. Simoneit (1994). "Hydrothermal pyrolysis of organic matter in Guaymas Basin: I. Comparison of hydrocarbon distributions in subsurface sediments and seabed petroleums." Organic Geochemistry **22**(6): 947-978.

Kellermann, M. Y., G. Wegener, M. Elvert, M. Y. Yoshinaga, Y.-S. Lin, T. Holler, X. P. Mollar, K. Knittel and K.-U. Hinrichs (2012). "Autotrophy as a predominant mode of carbon fixation in anaerobic methane-oxidizing microbial communities." Proceedings of the National Academy of Sciences **109**(47): 19321-19326.

Kubota, K., Y. Morono, M. Ito, T. Terada, S. Itezono, H. Harada and F. Inagaki (2014). "Gold-ISH: A nano-size gold particle-based phylogenetic identification compatible with NanoSIMS." Systematic and Applied Microbiology **37**(4): 261-266.

Lardin, H. A., R. R. Squires and P. G. Wenthold (2001). "Determination of the electron affinities of α-and β-naphthyl radicals using the kinetic method with full entropy analysis. The C—H bond dissociation energies of naphthalene." Journal of mass spectrometry **36**(6): 607-615.

Lechene, C., F. Hillion, G. McMahon, D. Benson, A. M. Kleinfeld, J. P. Kampf, D. Distel, Y. Luyten, J. Bonventre, D. Hentschel, K. M. Park, S. Ito, M. Schwartz, G. Benichou and G. Slodzian (2006). "High-resolution quantitative imaging of mammalian and bacterial cells using stable isotope mass spectrometry." Journal of Biology **5**(6): 20.

Lizarralde, D., A. Teske, T. W. Höfig, A. González-Fernández and t. I. E. Scientists (2023). "Carbon released by sill intrusion into young sediments measured through scientific drilling." Geology **51**(4): 329-333.

Lovley, D. R. and E. J. Phillips (1987). "Competitive mechanisms for inhibition of sulfate reduction and methane production in the zone of ferric iron reduction in sediments." Applied and Environmental Microbiology **53**(11): 2636-2641.

Lovley, D. R., J. D. Coates, J. C. Woodward and E. Phillips (1995). "Benzene oxidation coupled to sulfate reduction." Applied and Environmental Microbiology **61**(3): 953-958.

Meckenstock, R. U., E. Annweiler, W. Michaelis, H. H. Richnow and B. Schink (2000). "Anaerobic Naphthalene Degradation by a Sulfate-Reducing Enrichment Culture." Applied and Environmental Microbiology **66**(7): 2743-2747.

Meckenstock, R. U. and H. Mouttaki (2011). "Anaerobic degradation of non-substituted aromatic hydrocarbons." Current Opinion in Biotechnology **22**(3): 406-414.

Morono, Y., T. Terada, M. Nishizawa, M. Ito, F. Hillion, N. Takahata, Y. Sano and F. Inagaki (2011). "Carbon and nitrogen assimilation in deep subseafloor microbial cells." Proceedings of the National Academy of Sciences **108**(45): 18295-18300.

Morono, Y. and F. Inagaki (2016). "Analysis of low-biomass microbial communities in the deep biosphere." Advances in Applied Microbiology **95**: 149-178.

Morono, Y., M. Ito, T. Hoshino, T. Terada, T. Hori, M. Ikehara, S. D'Hondt and F. Inagaki (2020). "Aerobic microbial life persists in oxic marine sediment as old as 101.5 million years." Nature Communications **11**(1): 3626.

Morono, Y. (2023). "Accessing the energy-limited and sparsely populated deep biosphere: achievements and ongoing challenges of available technologies." Progress in Earth and Planetary Science **10**(1): 18.

Musat, F., A. Galushko, J. Jacob, F. Widdel, M. Kube, R. Reinhardt, H. Wilkes, B. Schink and R. Rabus (2009). "Anaerobic degradation of naphthalene and 2-methylnaphthalene by strains of marine sulfate-reducing bacteria." Environmental Microbiology **11**(1): 209-219.

Nagakura, T., F. Schubert, D. Wagner, J. Kallmeyer and I. E. S. S. P. (2022). "Biological Sulfate Reduction in Deep Subseafloor Sediment of Guaymas Basin." Frontiers in Microbiology **13**.

Orphan, V. J., C. H. House, K.-U. Hinrichs, K. D. McKeegan and E. F. DeLong (2001). "Methane-Consuming Archaea Revealed by Directly Coupled Isotopic and Phylogenetic Analysis." Science **293**(5529): 484-487.

Parkes, R. J., B. Cragg, E. Roussel, G. Webster, A. Weightman and H. Sass (2014). "A review of prokaryotic populations and processes in sub-seafloor sediments, including biosphere:geosphere interactions." Marine Geology **352**: 409-425.

Ramsay, J. A., H. Li, R. S. Brown and B. A. Ramsay (2003). "Naphthalene and Anthracene Mineralization Linked to Oxygen, Nitrate, Fe(III) and Sulphate Reduction in a Mixed Microbial Population." Biodegradation **14**(5): 321-329.

Rueter, P., R. Rabus, H. Wilkest, F. Aeckersberg, F. A. Rainey, H. W. Jannasch and F. Widdel (1994). "Anaerobic oxidation of hydrocarbons in crude oil by new types of sulphate-reducing bacteria." Nature **372**(6505): 455-458.

Schippers, A., L. N. Neretin, J. Kallmeyer, T. G. Ferdelman, B. A. Cragg, R. John Parkes and B. B. Jørgensen (2005). "Prokaryotic cells of the deep sub-seafloor biosphere identified as living bacteria." Nature **433**(7028): 861-864.

Shin, B., M. Kim, K. Zengler, K.-J. Chin, W. A. Overholt, L. M. Gieg, K. T. Konstantinidis and J. E. Kostka (2019). "Anaerobic degradation of hexadecane and phenanthrene coupled to sulfate reduction by enriched consortia from northern Gulf of Mexico seafloor sediment." Scientific Reports **9**(1): 1239.

Teske, A., A. V. Callaghan and D. E. LaRowe (2014). "Biosphere frontiers of subsurface life in the sedimented hydrothermal system of Guaymas Basin." Frontiers in Microbiology **5**.

Teske, A., D. Lizarralde, T. Höfig, I. Aiello, J. Ash, D. Bojanova, M. Buatier, V. Edgcomb, C. Galerne and S. Gontharet (2021a). "Expedition 385 summary." Proceedings of the International Ocean Discovery Program.

Teske, A., D. Lizarralde, T. Höfig, I. Aiello, J. Ash, D. Bojanova, M. Buatier, V. Edgcomb, C. Galerne and S. Gontharet (2021b). Site U1545. Guaymas Basin Tectonics and Biosphere, International Ocean Discovery Program.

Teske, A., D. Lizarralde, T. Höfig, I. Aiello, J. Ash, D. Bojanova, M. Buatier, V. Edgcomb, C. Galerne and S. Gontharet (2021c). Site U1546. Guaymas Basin Tectonics and Biosphere, International Ocean Discovery Program.

Thauer, R. K. and S. Shima (2008). "Methane as fuel for anaerobic microorganisms." Annals of the New York Academy of Sciences **1125**(1): 158-170.

Trembath-Reichert, E., Y. Morono, A. Ijiri, T. Hoshino, K. S. Dawson, F. Inagaki and V. J. Orphan (2017). "Methyl-compound use and slow growth characterize microbial life in 2-km-deep subseafloor coal and shale beds." Proceedings of the National Academy of Sciences **114**(44): E9206-E9215.

Trivedi, M. K., A. Branton, D. Trivedi, G. Nayak, P. Panda and S. Jana (2016). "Determination of isotopic abundance of 13C/12C or 2H/1H and 18O/16O in biofield energy treated 1-chloro-3-nitrobenzene (3-CNB) using gas chromatography-mass spectrometry." Science Journal of Analytical Chemistry **4**(4): 42-51.

Tsai, J.-C., M. Kumar and J.-G. Lin (2009). "Anaerobic biotransformation of fluorene and phenanthrene by sulfate-reducing bacteria and identification of biotransformation pathway." Journal of Hazardous Materials **164**(2): 847-855.

Wagner, M. (2009). "Single-Cell Ecophysiology of Microbes as Revealed by Raman Microspectroscopy or Secondary Ion Mass Spectrometry Imaging." Annual Review of Microbiology **63**(1): 411-429.

Wellsbury, P., K. Goodman, T. Barth, B. A. Cragg, S. P. Barnes and R. J. Parkes (1997). "Deep marine biosphere fuelled by increasing organic matter availability during burial and heating." Nature **388**(6642): 573-576.

Widdel, F. and F. Bak (1992). Gram-negative mesophilic sulfate-reducing bacteria. The prokaryotes, Springer**:** 3352-3378.

Williams, P. (1985). "Secondary ion mass spectrometry." Annual Review of Materials Science **15**(1): 517-548.

Zhang, X. and L. Y. Young (1999). "Carboxylation as an Initial Reaction in the Anaerobic Metabolism of Naphthalene and Phenanthrene by Sulfidogenic Consortia." Applied and Environmental Microbiology **65**(5): 2279-2279.